Eur Phys J A (2005) **24,** s1, 85–89
DOI: 10.1140/epjad/s2005-05-015-9

EPJ A direct
electronic only

Two-step rescattering in (e,e'p) reactions

C. Barbieri[1], L. Lapikás[2], and D. Rohe[3]

[1] TRIUMF, 4004 Wesbrook Mall, Vancouver, British Columbia, Canada V6T 2A3, e-mail: barbieri@triumf.ca
[2] NIKHEF, P.O. Box 41882, 1009 DB Amsterdam, The Netherlands
[3] University of Basel, CH-4056, Switzerland

Received: 26 September 2004 / Published Online: 8 February 2005

Abstract. This contribution reviews a calculation of two-step rescattering events in $(e, e'p)$ reactions. A semiclassical approach is employed for different kinematics, involving both medium and large missing energies. The effects of nuclear transparency and Pauli blocking are also included. The results are of interest for experiments aimed to study short-range correlations in the spectral distribution and suggest that the effects of rescattering can be strongly reduced in parallel kinematics. The comparison with the experimental data seem to confirm that sensible measurements could be achievable with a careful choice of the kinematics. However, contributions to final state interactions beyond the ones considered here become relevant for heavy nuclei. For transverse kinematics, rescattering induce large shifts of the spectral strength that can lead to a total experimental yield much larger than the direct signal.

TRIUMF preprint: TRI-PP-04-18

PACS. 25.30.Fj – 25.30.Dh

1 Introduction

Short range correlations (SRC) have long been known to be one of the major elements influencing the dynamics of nuclear systems [1,2]. Their main effects consist in shifting a sizable amount of spectral strength, about 10-15% [3], to very high missing energies and momenta. This results in an equally large depletion of the deeply bound orbitals, which is fairly independent of the given subshell and of the nuclear radius. Several theoretical studies have suggested that most of the missing strength is found along a ridge in the momentum-energy plane (p_m-E_m) which spans several hundreds of MeV/c (and MeV) [4,5,6,7]. This distribution is also responsible for most of the binding energy of nuclear systems [8]. The main characteristics of these results appear to be confirmed by recent experimental data [9,7], which will be also considered further below.

Due to the importance of SRC effects, measurements of the correlated tail have been attempted in the past. This was done by means of $(e, e'p)$ reactions. Unfortunately, these studies gave limited results due to the enormous background that is generated by final state interactions (FSI), see for example [10,11]. Several attempts to compute the latter were done by different groups [12,13,14,15,16]. In general, theory predicts larger effects when the transverse momentum distribution is considered. Interference effects between FSI and SRC correlations can also play a role [17,15]. The results of [13,18] suggests that multiple rescattering contributions (more than two-steps)

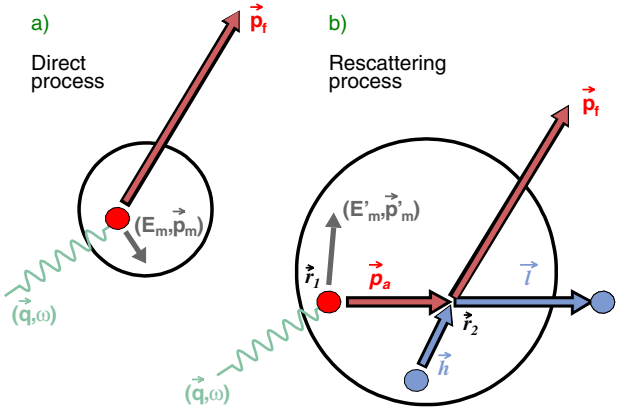

Fig. 1. Schematic representation of the direct knockout of a proton (**a**), given by the PWIA, and the contribution from a two-step rescattering (**b**). In the latter a proton or neutron is emitted with momentum $\mathbf{p}_a$ and different missing momentum and energy $(\mathbf{p}'_m, E'_m)$. Due to a successive collision, a proton is eventually detected with the same momentum $\mathbf{p}_f$ as seen in the direct process

are relatively small in light nuclei like ^{12}C but can become relevant for heavy systems. However, all these effects were seen to be reduced in parallel kinematics (that are defined here in terms of the angle between the momentum transferred by the electron $\mathbf{q}$ and the missing momentum

$\mathbf{p}_m$ [1]). The issue of how to minimize the FSI in $(e,e'p)$ experiments has been recently addressed in [19]. There, it was suggested that for properly chosen kinematics FSI are dominated by two-step rescattering processes like the one depicted in Fig. 1. In agreement with the above considerations, rescattering effects become particularly relevant when regions of small spectral strength are probed in perpendicular kinematics. A study of several kinematic conditions shows that the rescattered nucleons can move spectral strength in the p_m-E_m plane, from the top of the ridge toward regions where the correlated strength is small, therefore submerging the direct signal in a large background noise. Other possible contributions that involve the excitation of a Δ resonance are expected to be more sensitive to transverse degrees of freedom. Parallel kinematics tend to be more clean due to the high momentum that is required for the detected proton. New data were subsequently taken in these conditions by the E97-006 collaboration at Jefferson Lab [20,9,7] for a set of nuclei ranging from carbon to gold.

A different experiment has been undertaken recently at NIKHEF to measure the spectral function for the complete mean field region of ^{208}Pb [21]. This gave information of the above mentioned depletion of deeply bound orbitals and required probing medium missing energies, up to E_m=110 MeV. In [21], the scattered proton was detected at energies at which a full distorted wave calculation, in terms of an optical potential, is required. However, rescattering processes leading to the emission of two nucleons (one of which is not detected) can lead to the reappearance of part of the experimental strength absorbed by inelastic processes. This reaction mechanism is analogous to the one pointed out in [19] and Fig. 1 and was investigated in terms of a semiclassical model, inspired by the work of [22]. In these proceedings, we review the results obtained with this approach in [23] for both the NIKHEF and the E97-006 experiments.

2 The model

We consider contributions to the experimental yield that come from two-step mechanisms in which a reaction $(e,e'a)$ is followed by a scattering process from a nucleon in the medium, $N'(a,p)N''$, eventually leading to the emission of the detected proton and the undetected nucleon N''. For the present work, a may represent either a proton (with $N'=p$ or n) or a neutron (three channels in total). The letter a will also be used to label the possible open channels. The semi-exclusive cross section for these events was calculated according to [23,21]. By summing over the possible channels,

$$\frac{d^6\ \sigma_{rescatt.}}{dE_0\ d\Omega_{\hat{k}_o} dE_f\ d\Omega_{\hat{p}_f}} = \sum_a \int d\mathbf{r}_1 \int d\mathbf{r}_2 \int_0^\omega dT_a \times\rho_N(\mathbf{r}_1)\ \frac{K\ S_a^h(p'_m,E'_m)\ \sigma_{ea}^{cc1}}{M\ (\mathbf{r}_1-\mathbf{r}_2)^2} g_{aN'}(|\mathbf{r}_1-\mathbf{r}_2|) \quad (1)$$
$$\times P_T(p_a;\mathbf{r}_1,\mathbf{r}_2)\rho_{N'}(\mathbf{r}_2)\ \frac{d^3\ \sigma_{aN'}}{dE_f\ d\Omega_{\hat{p}_f}}\ P_T(p_f;\mathbf{r}_2,\infty)\ ,$$

where $(E_o,\mathbf{k}_o)$ and $(E_f,\mathbf{p}_f)$ represent the four-momenta of the detected electron and proton, respectively. Equation (1) assumes that the intermediate particle a is generated in plane wave impulse approximation (PWIA) by the electromagnetic current at a point $\mathbf{r}_1$ inside the nucleus. Here $K=|\mathbf{p}_a|E_a$ is a phase space factor, $S_a^h(p'_m,E'_m)/M$ is the spectral function of the hit particle a normalized to one [i.e., $M=N(Z)$ if a is a neutron (proton)] and σ_{ea}^{cc1} the off shell electron-nucleon cross section, for which we have used the $cc1$ prescription of de Forest [24]. The pair distribution functions $g_{aN'}(|\mathbf{r}_1-\mathbf{r}_2|)$ account for the joint probability of finding a nucleon N' in $\mathbf{r}_2$ after the particle a has been struck at $\mathbf{r}_1$ [25]. The integration over the kinetic energy T_a of the intermediate particle a ranges from 0 to the energy ω transfered by the electron. The factor $P_T(p;\mathbf{r}_1,\mathbf{r}_2)$ gives the transmission probability that the struck particle a propagates, without any interactions, to a second point $\mathbf{r}_2$, where it scatters from the nucleon N' with cross section $d^3\ \sigma_{aN'}$. The whole process is depicted in Fig. 1b.

The in medium cross section $d^3\ \sigma_{aN'}$ is obtained by adding the constraints of Pauli blocking to the nucleon-nucleon (NN) cross section and accounting for the Fermi distribution of the hit nucleon [23]. The NN differential cross section for small and large energies was extracted from the SAID data base [26] or expressed in terms of a small angle parameterization, respectively. This approach is accurate at large nucleon momenta, since the interaction with the medium becomes weak in this regime. In the kinematics of [21], protons are scattered with energies of about 100–250 MeV and the dispersion effects of the medium also need to be accounted for. These were added in terms of the effective Dirac mass and the time-like part of a vector potential U_V, which were computed in [27] using Dirac-Brueckner-Hartree-Fock theory. In doing this, a further constraint was imposed that the undetected nucleon is scattered into the continuum.

3 Results

The studies of [21], employed two different parallel kinematics in which the outgoing proton was emitted in the same direction as the momentum transfer (thus $\mathbf{q}$ and $\mathbf{p}_m$ were also parallel). The central kinetic energy of the outgoing proton was kept constant at 161 MeV (p_f =570 MeV/c) in both cases. The two kinematics differ only for the energy of the electron beam, which was taken to be E_o^H =674 MeV for the first case and E_o^L =461 MeV for the other. These choices correspond to a Q^2 ranging between 0.08 and 0.22 GeV^2. The spectral function of ^{208}Pb was extracted for missing energies up to 110 MeV and parametrized in terms of single particle orbitals spread in energy.

[1] With this nomenclature 'perpendicular' and 'transverse' kinematics have the same meaning. This definition becomes useful in the limit of high momentum transfer, where $\mathbf{q}$ and $\mathbf{p}_f$ always tend to be collinear.

The same parameterization was used as input spectral function in (1) and calculations were performed with the same kinematics, in order to estimate the importance of possible contributions from two-nucleon emissions. Figure 2 plots the results after they have been converted to a reduced representation by dividing them by $|p_f E_f|T\sigma_{eN}^{cc1}$ (where T is the nuclear transparency). These are compared to the input spectral function. The yield resulting from rescattering is between one and two orders of magnitude smaller than the direct signal, except for low missing momenta and missing energies above 60 MeV, where it gives a correction of about 20%. The rescattering effects are also found to be independent on which of the above kinematics is chosen. In practice this means that the ratio rescattering yield/direct yield does not depend on the longitudinal-transverse character of the exchanged virtual photon. These findings support an analysis of data in [21] based on standard distorted wave calculations.

In [9] data were taken in both parallel and perpendicular kinematics with the aim of investigating the reaction mechanism. In the first case, the angle between the photon and the initial momentum ($-\mathbf{p}_m$) was chosen to be $\vartheta_{qpi} \sim 20$ deg and the energy of the proton was $E_f \geq\sim 1.8$ GeV [20]. For the perpendicular kinematics, $\vartheta_{qpi} \sim 90$ deg and $E_f \sim 1.3$ GeV. In both cases the four momentum transfered by the electron was $Q^2 \sim 0.40$ GeV^2. The energy of the scattered nucleons is large enough that only the effects of Pauli blocking are relevant in the calculation of $d^3\ \sigma_{aN'}$. These kinematics are sensitive to the SRC tail at very large missing energies and momenta. Thus it is convenient to split the spectral function as the sum of a mean field and a correlated part,

$$S^h(p_m, E_m) = S^h_{MF}(p_m, E_m) + S^h_{corr}(p_m, E_m)\ , \qquad (2)$$

where $S^h_{corr}(p_m, E_m)$ is the strength directly probed by the experiment and was parametrized as

$$S^h_{corr}(p_m, E_m) = \frac{C\ e^{-\alpha\, p_m}}{[E_m - e(p_m)]^2 + [\Gamma(p_m)/2]^2} \qquad (3)$$

where $e(p_m)$ and $\Gamma(p_m)$ are smooth functions of the missing momentum, fitted to the available ^{12}C$(e, e'p)$ data in parallel kinematics [7]. This is shown by solid line in Figs. 3 and 4. The calculation with a ^{197}Au target employed the same S^h_{corr} of (3) multiplied by 79/6 or 118/6 to account for the correct number of protons and neutrons, respectively. Most of the remaining strength, $S^h_{MF}(p_m, E_m)$, is localized in the mean field orbitals. For ^{12}C these have been extracted from the world data in [28]. Since no direct data is available for ^{197}Au we choose to employ the spectral function discussed above for ^{208}Pb [21] properly normalized to the number of protons and neutrons of gold.

Due to the loss of energy of the ejected nucleon at the rescattering vertex, the spectral strength is always shifted toward higher missing energies. This is clearly visible in Fig. 3, where the results for the total reduced spectral function $[(d\sigma_{PWIA} + d\sigma_{rescatt.})/|p_f E_f|T\sigma_{eN}^{cc1}]$ are plotted for ^{12}C and ^{197}Au. The contribution to parallel kinematics is negligible at missing energies below the peak of the correlated tail but it tends to become more important for

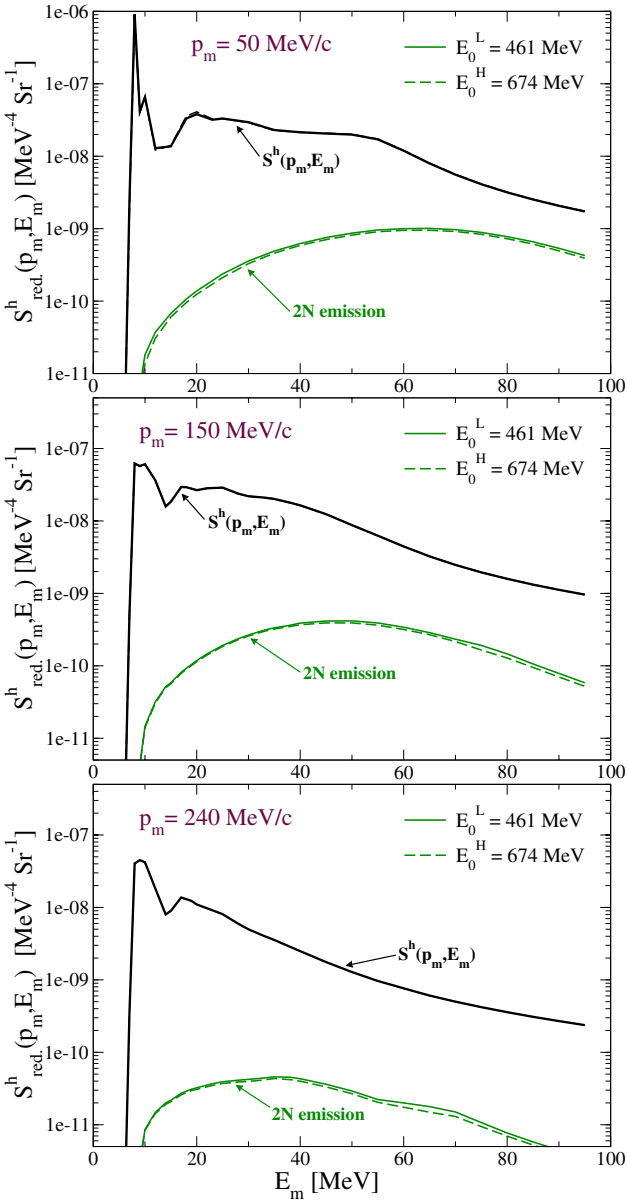

Fig. 2. Theoretical results for the rescattering contribution to the reduced spectral strength of ^{208}Pb for the kinematics of [21]. The *full* (*dashed*) *lines* refer to the kinematics with lower (E_o^L) and higher (E_o^H) energy beams. The *thick lines* shows the input spectral function, $S^h_p(p_m, E_m)$

E_m >150–200 MeV. This confirms the expected trend that a part of the strength seen in this region is dragged from places where the hole spectral function is larger [19]. The same behavior is seen in perpendicular kinematics where, however, rescattering effects are already relevant at small missing energies. In this situation the direct process accounts for only 30–50% of the total yield obtained at the top of the correlated peak. At higher energies, the rescattering can overwhelm the PWIA signal by more than an order of magnitude. It should be noted that for both parallel and perpendicular kinematics the contribution of (1) tends to increase with the nuclear radius.

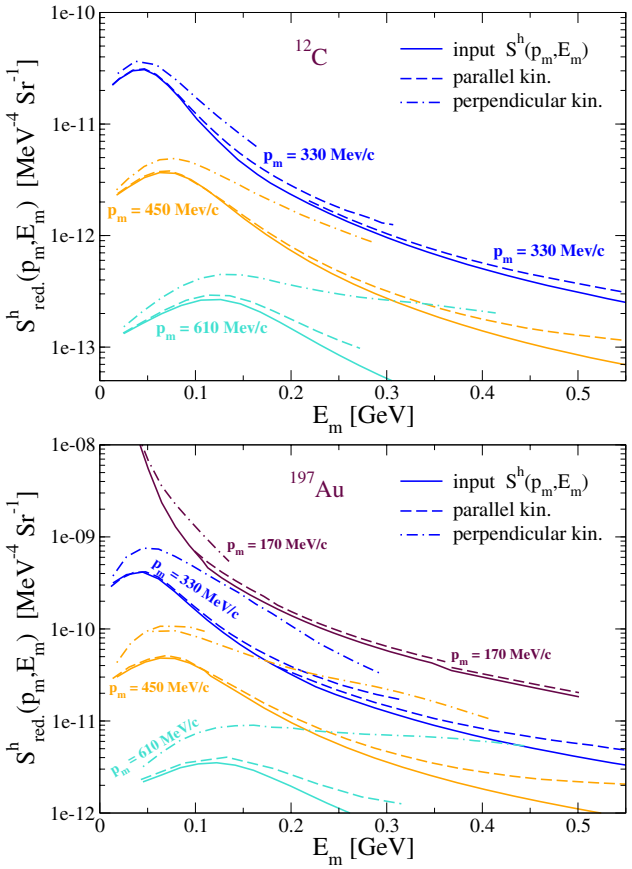

Fig. 3. Theoretical results for the reduced spectral strength in the correlated region obtained in parallel (*dashed line*) and perpendicular (*dot-dashed line*) kinematics. The *full line* shows the model spectral function, (2), employed in the calculations. The results are shown for ^{12}C (*top*) and ^{197}Au (*bottom*) targets

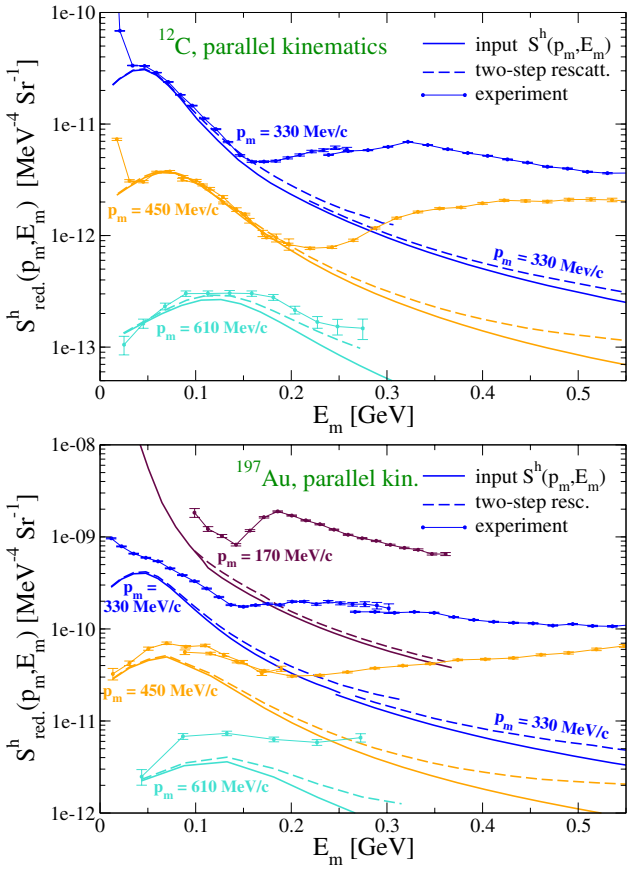

Fig. 4. Theoretical results for the total reduced spectral strength (*dashed line*) are compared to the experimental data in parallel kinematics. The *full line* shows the model spectral function, (2), employed in the calculations. The *top* (*bottom*) panel refer to a ^{12}C (^{197}Au) target and the experimental data are from [20]. The values of p_m refer to the center of the experimental bins

In [9] the strength seen by the E97-006 experiment was integrated over a part of the correlated region in the p_m-E_m plane. For ^{12}C and parallel kinematics the total amount of protons seen in this area was found to agree with theoretical predictions. This is in line with the above results that predict very small rescattering contributions at the top of the correlated ridge for these kinematics. Thus, it supports the above choice of fitting (3) to the experiment. The quality of this fit is shown by the top panel of Fig. 4. As the missing energy increases, (3) decreases in a realistic way. However, the experimental cross section is substantially enhanced above $E_m \sim 150$ MeV, which is the threshold for $(e, e'p\pi)$ events. At very high energies other mesons can be produced and the experimental cross section tends to become flat. Here, the yield is at least one order of magnitude larger than the direct signal and calculated rescattering events represent a minor contribution to the total FSI.

The results for gold are compared to the experiment in parallel kinematics in the bottom panel of Fig. 4. In this case the spectral function (2) is the same used for ^{12}C but normalized according to the different number of protons of ^{197}Au. While, this is only a first approximation it is clear that an analogous fit of (3) to the experimental data for ^{197}Au would imply an unrealistically large number of protons in the correlated tail. Thus the discrepancy between theory and experiment should be considered as evidence that in heavy nuclei the FSI effects beyond two-step rescattering are present already in the correlated region. At very large E_m the experiment has the same behavior as observed for ^{12}C. However, the valley between the correlated and pion emission regions is completely filled due to FSI effects.

4 Summary

Probing the effects of SRC in $(e, e'p)$ experiments requires measurements of the spectral function at large missing energies. This requires kinematical conditions in which the effects of final state interaction can be very complicated and can lead to a large contribution to the experimental yield. Thus, they would overwhelm the direct signal. However, these effects strongly depend on the particular kinematics chosen. This paper considers a semiclassical model of two-step rescattering events, which represents a

first approximation to FSI, and applies it to investigate its consequences for the kinematics of two different experiments.

For kinematics involving outgoing protons of the order of few hundreds of MeV, the present model was employed to estimate the reappearance of strength through inelastic channels that lead to two-nucleon emission. In the reaction $^{208}\mathrm{Pb}(e,e'p)$ the overall effects were seen to be about an order of magnitude or more smaller than the direct signal. This supports an analysis of the experimental data based on usual distorted wave calculations.

Further calculations were performed for both the parallel and perpendicular kinematics employed in the E97-006 experiment at JLab that focused on the SRC distributions at high missing energies and momenta. Calculations were performed for ^{12}C and ^{197}Au targets, which have different radii. In general, rescattering is found to be much smaller in parallel kinematics than in perpendicular ones. The comparison with the experimental data in parallel kinematics suggests that the rescattering contribution to FSI is calculable with reasonable accuracy in this case. For ^{12}C it is suggested that the effects of FSI are small for missing energies below ∼150 MeV. Above that the effects of pion emission become dominant. For ^{197}Au FSI effects beyond two-step rescattering are important even in parallel kinematics.

Acknowledgements. This work is supported by the Natural Sciences and Engineering Research Council of Canada (NSERC) and by the "Stichting voor Fundamenteel Onderzoek der Materie (FOM)", which is financially supported by the "Nederlandse Organisatie voor Wetenschappelijk Onderzoek (NWO)" and by the "Schweizerische Nationalfonds (NSF)".

References

1. V.R. Pandharipande, I. Sick, P.K.A. deWitt Huberts: Rev. Mod. Phys. **69**, 981 (1997)
2. W.H. Dickhoff, C. Barbieri: Prog. Part. Nucl. Phys. **52**, 377 (2004)
3. B.E. Vonderfecht, W.H. Dickhoff, A. Polls, A. Ramos: Phys. Rev. C **44**, R1265 (1991)
4. C. Ciofi degli Atti, S. Liuti, S. Simula: Phys. Rev. C **41**, R2474 (1990)
5. O. Benhar, A. Fabrocini, S. Fantoni, I. Sick: Nucl. Phys. A **579** 493 (1994)
6. H. Müther, W.H. Dickhoff: Phys. Rev. C **49**, R17 (1994); H.Müther, W.H. Dickhoff, A. Polls: Phys. Rev. C **51**, 3040 (1995)
7. T. Frick, K.S.A. Hassaneen, D. Rohe, H. Müther: Phys. Rev. C. **70**, 024309 (2004)
8. Y. Dewulf, W.H. Dickhoff, D. Van Neck, E.R. Stoddard, M. Waroquier: Phys. Rev. Lett. **90**, 152501 (2003)
9. D. Rohe, et al.: nucl-ex/0405028; To be published on Phys. Rev. Lett.
10. R.W. Lourie, et al.: Phys. Rev. Lett. **56**, 2364 (1986)
11. H. Baghaei, et al.: Phys. Rev. C **39**, 177 (1989); L.B. Weinstein, et al.: Phys. Rev. Lett. **64**, 1646 (1990)
12. T. Takaki: Phys. Rev. Lett. **62**, 395 (1989)
13. P. Demetriou, S. Boffi, C. Giusti, F.D. Pacati: Nucl. Phys. A **625**, 513 (1997)
14. N.N. Nicolaev, et al.: Nucl. Phys. A **582**, 665 (1995)
15. H. Morita, C. Ciofi degli Atti, T. Treleani: Phys. Rev. C **60**, 034603 (1999)
16. S. Janssen, J. Ryckebusch, W. Van Nespen, D. Debruyne, Nucl. Phys. A **672**, 285 (2000)
17. A. Bianconi, S. Jeschonnek, N.N. Nicolaev, B.G. Zakharov: Nucl. Phys. A **608**, 437 (1996)
18. J. Ryckebusch, D. Debruyne, P. Lava, S. Janssen, B. Van Overmeire, T. Van Cauteren: Nucl. Phys. A **728**, 226 (2003)
19. I. Sick et al.: Jlab-Proposal E97-006 (1997)
20. D. Rohe: Eur. Phys. J. A **17**, 439 (2003), (*Conference proceeding on Electron-Nucleus Scattering VII in Elba 2002*); D. Rohe, Habilitationsschrift, University of Basel, 2004 (unpublished)
21. M.F. van Batenburg: Ph.D. Thesis, University of Utrecht, 2001
22. V.R. Pandharipande, S.C. Pieper: Phys. Rev. C **45**, 791 (1992)
23. C. Barbieri, L. Lapikás: nucl-th/0409032; submitted to Phys. Rev. C
24. T. de Forest, Jr.: Nucl. Phys. A **392**, 232 (1983)
25. R. Schiavilla, D.S. Lewart, V.R. Pandharipande, S.C. Pieper: R.B. Wiringa, S. Fantoni: Nucl. Phys. A **473**, 267 (1987)
26. R.A. Arndt, I.I. Strakovsky, R.L. Workman: Phys. Rev. C **62**, 034005 (2000); SAID data base web site: http://gwdac.phys.gwu.edu.
27. R. Brockmann, R. Machleidt: Phys. Rev. C **42**, 1965 (1990)
28. L. Lapikás, G. van der Steenhoven, L. Frankfurt, M. Strikman, M. Zhalov: Phys. Rev. C **61**, 064325 (2000)